第 45 卷 第 10 期
2024年 10 月

发 光 学 报
CHINESE JOURNAL OF LUMINESCENCE

Vol. 45 No. 10
Oct., 2024

Article ID: 1000-7032(2024)10-1639-08

Optical Properties of GaAs/AlGaAs Nanowires Grown on Pre-etched Si Substrates

ZHANG Zhihong[1,2], MENG Bingheng[1], WANG Shuangpeng[2], KANG Yubin[3*], WEI Zhipeng[1*]

(1. *State Key Laboratory of High Power Semiconductor Lasers, Changchun University of Science and Technology, Changchun* 130022, *China*;
2. *Instituted of Applied Physics and Materials Engineering, University of Macau, Macau* 999078, *China*;
3. *College of Optics and Electronic Science and Technology, China Jiliang University, Hangzhou* 310018, *China*)
* *Corresponding Authors, E-mail*: *kangyubin@cjlu. edu. cn*; *zpweicust@126. com*

Abstract: GaAs-based nanomaterials are essential for near-infrared nano-photoelectronic devices due to their exceptional optoelectronic properties. However, as the dimensions of GaAs materials decrease, the development of GaAs nanowires (NWs) is hindered by type-Ⅱ quantum well structures arising from the mixture of zinc blende (ZB) and wurtzite (WZ) phases and surface defects due to the large surface-to-volume ratio. Achieving GaAs-based NWs with high emission efficiency has become a key research focus. In this study, pre-etched silicon substrates were combined with GaAs/AlGaAs core-shell heterostructure to achieve GaAs-based NWs with good perpendicularity, excellent crystal structures, and high emission efficiency by leveraging the shadowing effect and surface passivation. The primary evidence for this includes the prominent free-exciton emission in the variable-temperature spectra and the low thermal activation energy indicated by the variable-power spectra. The findings of this study suggest that the growth method described herein can be employed to enhance the crystal structure and optical properties of other Ⅲ-Ⅴ low-dimensional materials, potentially paving the way for future NW devices.

Key words: GaAs nanowires; GaAs/AlGaAs core-shell structure; crystal phase; optical property
CLC number: O482. 31 **Document code**: A **DOI**: 10. 37188/CJL. 20240199

预刻蚀硅衬底上生长的GaAs/AlGaAs纳米线的光学特性

张志宏[1,2], 孟兵恒[1], 王双鹏[2], 亢玉彬[3*], 魏志鹏[1*]

(1. 长春理工大学 高功率半导体激光国家重点实验室, 吉林 长春 130022;
2. 澳门大学 应用物理及材料工程研究院, 中国 澳门 999078;
3. 中国计量大学 光学与电子科技学院, 浙江 杭州 310018)

摘要: GaAs基纳米材料由于其出色的光电性能,对于近红外纳米光电子器件至关重要。然而,随着GaAs材料尺寸的缩小,由闪锌矿(ZB)和纤锌矿(WZ)相混合引起的Ⅱ-型量子阱结构和大的表面积体积比引起的表面缺陷严重阻碍了GaAs纳米线的发展。实现具有高发光效率的GaAs基纳米线已成为研究重点。本研究通过预刻蚀的硅衬底与形成GaAs/AlGaAs核壳异质结构相结合,利用阴影效应和表面钝化作用,制备了具有良好垂直性、优异晶体结构和高发光效率的GaAs基纳米线。这一结论的主要证据包括制备的GaAs基纳米线在变温光谱中突出的自由激子发射和变功率光谱中暗示的低热活化能。结果表明,所描述的生长方法可用于改善其他Ⅲ-Ⅴ低维材料的晶体结构和光学性能,有望为未来的纳米线器件奠定基础。

收稿日期: 2024-08-27; **修订日期**: 2024-09-02
基金项目: 国家自然科学基金(12074045,62027820,61904017); 吉林省自然科学基金(20230101352JC); 中国"111"项目(D17017)
Supported by National Natural Science Foundation of China(12074045,62027820,61904017); Natural Science Foundation of Jilin Province(20230101352JC); "111" Project of China(D17017)

关 键 词：GaAs纳米线；GaAs/AlGaAs核壳结构；晶相；光学特性

1 Introduction

In recent years, there has been considerable interest in researching low-dimensional semiconductors with a focus on nanoscale materials due to their demonstration of novel electrical and optical properties at smaller scales that hold promise for diverse optoelectronic applications[1-11]. Among the various Ⅲ-Ⅴ semiconductors, gallium arsenide (GaAs) shows considerable potential for its direct bandgap and tunable characteristics, particularly in infrared applications. In integrated nanophotonics, ultra-low power nanolasers are essential components to realizing key functionalities and prompt extensive investigations in the fields. However, from a materials preparation perspective, while GaAs thin films with a stable zinc blende (ZB) phase can be obtained *via* epitaxial growth, a metastable wurtzite (WZ) phase may emerge as the size decreases. The coexistence of these two phases not only increases crystal defects but also leads to the formation of type-Ⅱ quantum well structures, significantly diminishing emission efficiency[12-13]. Furthermore, upon dimension reduction, the significantly increased surface-to-volume ratio and numerous surface defects lead to a notable rise in surface recombination rate, further affecting the emission efficiency of GaAs nanowires (NWs)[14-15]. Therefore, despite the promising performance of GaAs NWs in various potential applications, improving their emission efficiency remains a prominent challenge in current scientific research.

Cutting-edge research reveals that wet chemical passivation can effectively reduce the surface state density by saturating dangling bonds on the GaAs surface, enhancing emission intensity without introducing new defect energy levels[14,16-19]. Common wet passivation methods include sulfur passivation and nitrogen passivation. However, the stability of improvement brought by wet passivation is not satisfactory for long-term storage and research. Additionally, the chemical treatment can contaminate the environment. Alternatively, surface passivation can also be achieved by growing an aluminum gallium arsenic (AlGaAs) shell layer, which offers two advantages. First, the core-shell nanostructure ensures long-term stability. Second, AlGaAs and GaAs form a type-Ⅰ energy band structure, facilitating charge carrier diffusion into the GaAs layer, thereby enhancing light absorption and ultimately boosting emission efficiency[20-22]. To tackle mixed phases in GaAs materials, optimizing growth parameters like growth temperature[23], Ⅴ/Ⅲ beam ratio[24], shear tension[25], epitaxial burying[26], annealing temperature[27], and doping[28] can control energy perturbations within a suitable growth range. Nevertheless, due to the narrow growth window and intricate control requirements, it is complicated to successfully prepare pure-phase structures. Moreover, scant focus has been directed towards substrate processing to govern nanowire phases and improve optical characteristics. In particular, the influence of substrate etching on the optical properties of the resulting NWs remains underexplored.

In a previous study, we suggested that pure ZB phase GaAs NWs could be produced by etching on silicon substrates with varying durations of natural oxide exposure[29]. However, deep-level defect luminescence persists in the optimized pure-phase GaAs NWs, significantly hindering their application in photonic devices. In this work, we introduce an AlGaAs shell layer on GaAs NWs grown on etched substrates, effectively suppressing defect-related emissions while maintaining the NW phase purity. Temperature- and power-dependent PL measurements demonstrate the successful fabrication of GaAs-based NWs with high crystal quality and emission efficiency. Our work provides valuable insights into achieving efficient luminescence in Ⅲ-Ⅴ semiconductors and supports the development of high-performance nano-optoelectronic devices.

2 Experiment

2.1 Molecular Beam Epitaxial Growth of NWs

The GaAs/AlGaAs core-shell NWs arrays were grown on Si substrate using a Ga-assisted self-catalyzed method with a DCA P600 molecular beam epitaxy system. Before growth, the Si substrates were ultrasonically cleaned with ethanol and deionized water. Expose the Si substrate to a 1∶10 buffered hydrofluoric acid solution for 3 s to eliminate the native SiO_2 layer and create nucleation sites, followed by drying using nitrogen gas. The control group was not subjected to substrate etching. Throughout the growth process, Ga droplets were applied as a catalyst by depositing them using a Ga beam equivalent pressure (BEP) of 8.3×10^{-6} Pa (6.2×10^{-8} Torr). The GaAs core NWs were grown at the same Ga BEP with an As BEP of 2.1×10^{-6} Pa (1.6×10^{-6} Torr). The Ⅴ/Ⅲ flux ratio was fixed at 26 during growth, with a growth time of 60 min. Following the completion of GaAs core NWs growth, AlGaAs shell structures were deposited. Al BEP of 5.9×10^{-6} Pa (4.4×10^{-8} Torr) was introduced to grow the AlGaAs shell, with a growth time of 30 min. The temperature was maintained at 620 ℃ throughout the growth. Finally, the GaAs/AlGaAs core-shell NWs were obtained.

2.2 Material Characteristics

The morphology of GaAs/AlGaAs NWs grown on both etched and unetched substrates was characterized by the scanning electron microscope (SEM, HITACHI S-4800). The NWs crystal structure was determined by TEM (FEI Tecnai G2-F20) using selected area electron diffraction (SAED) patterns. The optical properties of NWs were measured using a HORIBA iHR550 spectrometer equipped with an InGaAs detector. A 655 nm semiconductor diode laser with a spot diameter of approximately 7 mm was used as the excitation source. The laser power intensity was modulated by an attenuator and determined by an optical power meter. The PL spectra were measured on as-grown NW arrays.

3 Results and Discussion

As mentioned in the previous literature, the etching treatment of Si substrate could influence the relative content of WZ and ZB phases in GaAs-based NWs. The side-view SEM images in Fig. 1(a)-(b) clearly show that the GaAs/AlGaAs NWs grown before and after substrate etching are vertically

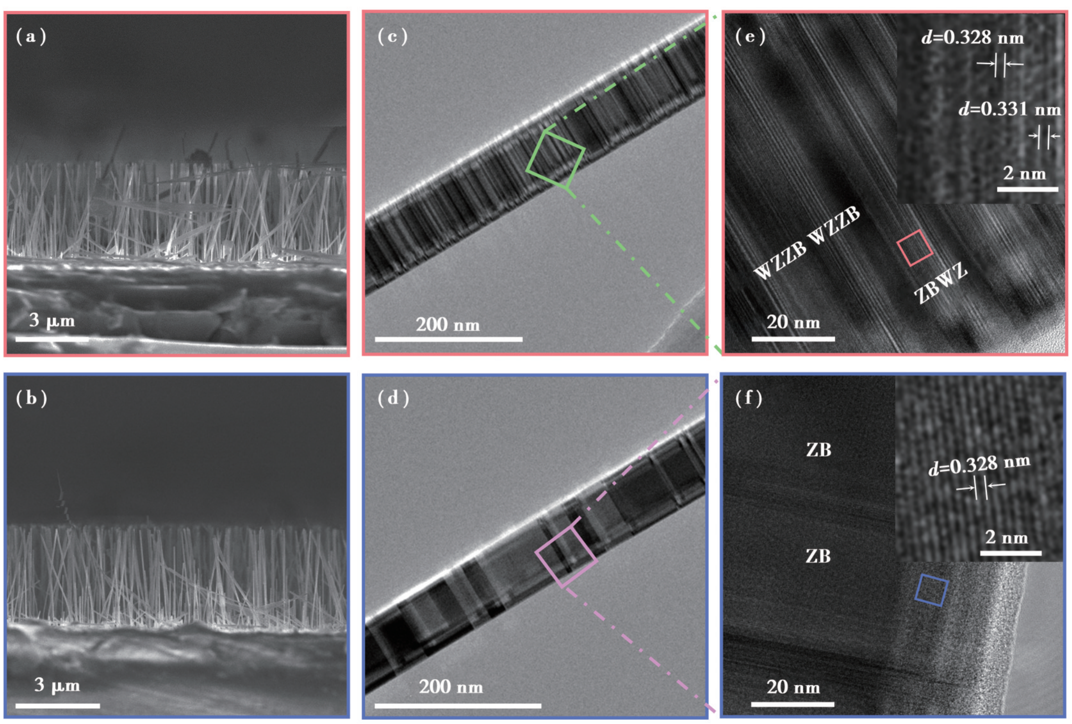

Fig.1 Morphological characterization of unetched(a) and etched(b) substrate side-view SEM images of the GaAs/AlGaAs core-shell NWs. (c)-(d) The TEM image shows unetched and etched GaAs/AlGaAs core-shell NW. (e)-(f) High-resolution TEM images of unetched and etched NWs, respectively

aligned on the Si substrate with high uniformity. The average diameters of the nanowire arrays before and after etching are 85 nm and 66 nm, respectively, with densities of 16.47/μm^2 and 23.95/μm^2. To visually characterize the crystalline phase in the GaAs-based NWs grown pre- and post-etching substrate, TEM characterization of the NWs in the two samples are performed respectively, with results shown in Fig. 1. Fig. 1(c)-(d) display the low-magnification images of core-shell NWs before and after substrate etching. Notably, regions with varying contrasts are visible along the NW direction. A closer inspection of the images near the NW core edges reveals that in NWs grown without substrate etching, the WZ and ZB phases are intermixed at high density, as shown in Fig. 1(e). In contrast, after etching the substrate, only the ZB phase is observed, as shown in Fig. 1(f). The WZ and ZB phases are identified by lattice spacing, as shown in the insets of Fig. 1(e)-(f). This can be attributed to the shadowing effect[29], which creats additional sites for nanowire self-catalyzed growth by etching the substrate. Moreover, the density of nanowire effectively regulates the Ⅴ/Ⅲ flux ratio during growth, resulting in nanowires with a pure ZB phase. Additionally, the observed shadowing effect, amplified by increased nanowire density, is consistent with our SEM test results.

The phase-pure nature of GaAs-based NWs can be further confirmed by their photoluminescence (PL) properties. Fig. 2 presents the normalized low-temperature (10 K) PL spectrum of NWs before and after substrate etching at an excitation power of 100 mW. For NWs grown on the unetched substrate, three distinct emission peaks are observed at 1.515 eV (P1), 1.496 eV (P2), and 1.488 eV (P3). As is well known, based on the peak positions, P1 represents free exciton emission, P2 may stem from type-Ⅱ quantum well emission induced by the WZ/ZB structure, and P3 likely originates from defect emission due to the mixed WZ and ZB phases or stacking faults within the WZ or ZB phases[30-31]. Interestingly, after substrate etching, the PL emission shows a notable absence of type-Ⅱ quantum well emission compared to the untreated sample. Concurrently, the relative emission intensity ratio between free excitons and defects increases significantly. These observations can be explained as follows: substrate etching influences the effective Ⅴ/Ⅲ flux ratio during NW growth, reducing the WZ phase content within the NWs[29]. Consequently, the distinct type-Ⅱ quantum well emission is not detected, and defect emission from the stacking faults of ZB phases is also significantly suppressed, leading to superior optical performance in the etched substrate sample.

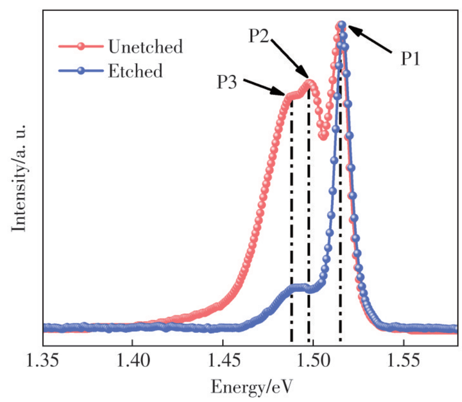

Fig.2 A comparative analysis of the optical properties of NWs before and after the process of substrate etching at 10 K

To further investigate the emission characteristics of GaAs/AlGaAs core-shell NWs before and after substrate etching, power-dependent PL measurements were conducted on the sample at 10 K. As depicted in Fig. 3(a), under 1 mW excitation power, no significant free exciton emission peak (P1) is observed in the NWs without etched substrates, with P2 and P3 emissions predominated. As the excitation power increases from 1 mW to 100 mW, a gradual blue shift in the emission peak of P2 is observed. This observation, combined with the TEM test results shown in Fig. 1, suggests that this emission peak originates from a type-Ⅱ quantum well. Regarding P3, as excitation power increases from 1 mW to 100 mW, its emission intensity relative to P1 gradually decreases due to the lower state density of defects compared to free excitons. Under identical experimental conditions, the emission in NWs grown on the etched substrate is dominated by P1, accompanied by defect luminescence related to stacking faults in the ZB phase, as shown in Fig. 3(b). This conclusion is further supported by the data in Fig. 1. Moreover, the ratio of free exciton to defect emission in NWs grown post-substrate etching surpasses that in unetched NWs throughout all power tests, as illustrated in Fig. 3(c). This implies that the optical properties of NWs grown after substrate etching are significantly improved.

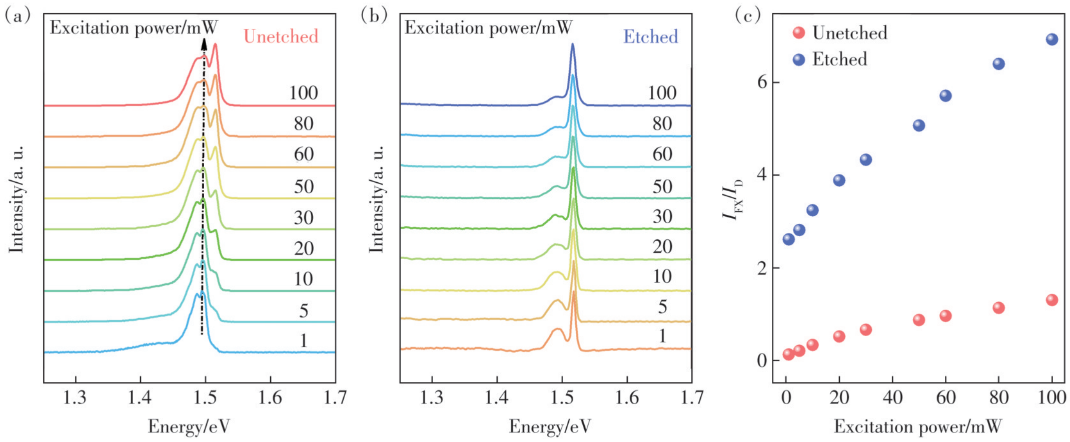

Fig.3　Evolution of the PL spectra measured at 10 K under different excitation powers. GaAs/AlGaAs NWs grown before(a) and after(b) substrate etching. (c) Variation of the relative PL peaks intensity ratio of free exciton and defect with excitation power

Next, we investigate the temperature dependence of PL emission from GaAs/AlGaAs NWs grown before and after substrate etching. As can be seen in Fig. 4(a)-(b), the PL intensity gradually decreases as the temperature increases. The temperature-dependent integrated PL intensity cannot be well fitted by a single thermally activated Arrhenius plot. However, it can be adequately described by a dual-activation energy model[32]:

$$I(T) = \frac{1}{1 + c_1\exp\left(-\frac{E_1}{k_B T}\right) + c_2\exp\left(-\frac{E_2}{k_B T}\right)}, \quad (1)$$

where E_1 and E_2 represent distinct activation energies for two different thermal activation processes, while the parameters c_1 and c_2 denote the relative ratios of non-radiative recombination. By fitting the temperature-dependent PL data to the dual activation energy model (Fig. 4(c)), we can extract the values of the two activation energies, which provide insights into the dominant recombination mechanisms in the NWs. Using the least-squares fitting procedure with Eq. 1, the activation energies obtained for the samples before substrate etching are 9.95 meV and 14.38

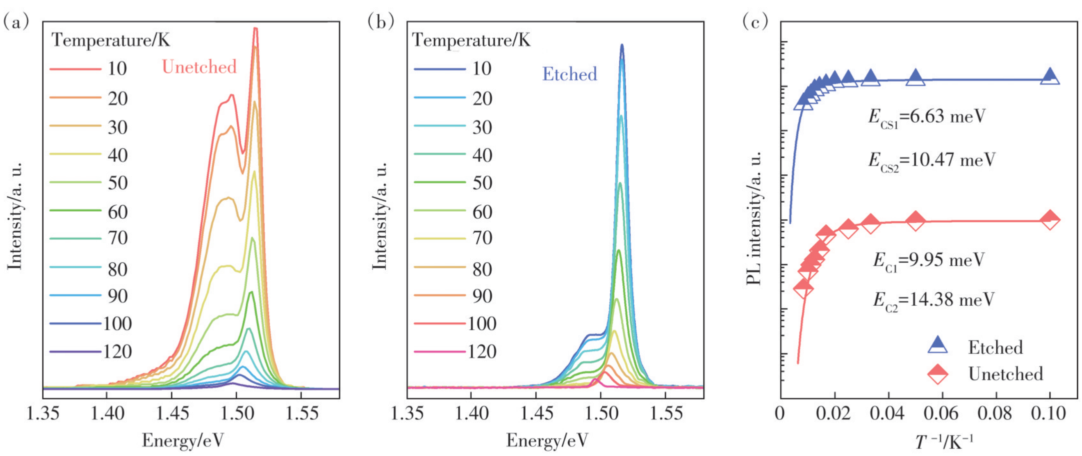

Fig.4　Temperature-dependent PL spectra of GaAs-based NWs. GaAs/AlGaAs NWs grown before(a) and after(b) substrate etching. (c) The dependence of the PL intensity on the reciprocal of temperature, and the solid curve is the Arrhenius fit with two activation energies

meV, respectively, whereas these values change to 6.63 meV and 10.47 meV. The smaller activation energy (E_1) in each case corresponds to the thermal energy required for free excitons to dissociate into continuum states. Notably, the obtained activation energies (6.63 meV and 9.95 meV) are comparable to the exciton binding energies of bulk GaAs (around 5 meV), which supports our assignment[33]. The larger activation energy (E_2) likely relates to the thermally activated capture of excitons by non-radiative defects within the GaAs/AlGaAs NWs. It is noteworthy that the activation energies for NWs grown on etched substrates are smaller than those for NWs grown on unetched substrates. This further confirms that substrate etching before growth helps eliminate internal defects and enhances the optical properties of GaAs-based NWs[34].

4 Conclusion

In conclusion, combining the substrate etching method with the growth of AlGaAs shell layers has proven to be an effective approach for GaAs-based NWs with high crystalline quality and emission efficiency. The nanowires fabricated pre- and post-etching underwent thorough characterization employing SEM, TEM, and PL analyses. Analysis of the experimental results demonstrates that the crystalline phase properties of GaAs/AlGaAs NWs can be optimized by regulating the etching process. Furthermore, combined power- and temperature-dependent PL results indicate that the nonradiative complexes in the NWs grown after etching are significantly reduced. This progress not only provides a reference for research on other semiconductor NWs but also facilitates the development of nanodevices.

Response Letter is available for this paper at:http://cjl.lightpublishing.cn/thesisDetails#10.37188/CJL.20240199.

References:

[1] ZHU X T, LIN F Y, ZHANG Z H, *et al*. Enhancing performance of a GaAs/AlGaAs/GaAs nanowire photodetector based on the two-dimensional electron-hole tube structure [J]. *Nano Lett.*, 2020, 20(4): 2654-2659.

[2] 李想, 亢玉彬, 唐吉龙, 等. Si掺杂对GaAs纳米线发光特性的影响[J]. 发光学报, 2021, 42(5): 629-634.
LI X, KANG Y B, TANG J L, *et al*. Effect of Si doping on photoluminescence properties of GaAs nanowires [J]. *Chin. J. Lumin.*, 2021, 42(5): 629-634. (in Chinese)

[3] SAXENA D, MOKKAPATI S, PARKINSON P, *et al*. Optically pumped room-temperature GaAs nanowire lasers [J]. *Nat. Photonics*, 2013, 7(12): 963-968.

[4] STETTNER T, ZIMMERMANN P, LOITSCH B, *et al*. Coaxial GaAs-AlGaAs core-multishell nanowire lasers with epitaxial gain control [J]. *Appl. Phys. Lett.*, 2016, 108(1): 011108.

[5] 于立新, 宋宏伟, 刘钟馨, 等. $LaPO_4$:Ce^{3+}/Tb^{3+}纳米线的合成和发光特性[J]. 发光学报, 2005, 26(3): 369-374.
YU L X, SONG H W, LIU Z X, *et al*. Preparation and luminescence properties of $LaPO_4$:Ce^{3+}/Tb^{3+} nanowires [J]. *Chin. J. Lumin.*, 2005, 26(3): 369-374. (in Chinese)

[6] ZHANG X T, YI R X, ZHAO B J, *et al*. Vertical emitting nanowire vector beam lasers [J]. *ACS Nano*, 2023, 17(11): 10918-10924.

[7] SCHREITMÜLLER T, JEONG H W, ESMAIELPOUR H, *et al*. Large tolerance of lasing properties to impurity defects in GaAs(Sb)-AlGaAs core-shell nanowire lasers [J]. *Adv. Funct. Mater.*, 2024, 34(12): 2311210.

[8] MENG B H, KANG Y B, ZHANG X Y, *et al*. Room-temperature near-infrared lasing from GaAs/AlGaAs core-shell nanowires based on random cavity [J]. *ACS Appl. Mater. Interfaces*, 2024, 16(31): 41677-41683.

[9] RASHIDI M, HAGGREN T, SU Z C, *et al*. Managing resonant and nonresonant lasing modes in GaAs nanowire random lasers [J]. *Nano Lett.*, 2021, 21(9): 3901-3907.

[10] RASHIDI M, HAGGREN T, JAGADISH C, *et al*. Characteristics and thermal control of random and Fabry-Pérot lasing in nanowire arrays [J]. *ACS Photonics*, 2022, 9(11): 3573-3583.

[11] 张楠, 谢启杰, 纳全鑫, 等. 硅基量子点激光器研究进展[J]. 发光学报, 2023, 44(11): 2011-2026.

ZHANG N, XIE Q J, NA Q X, *et al.* Research progress on silicon-based quantum dot lasers [J]. *Chin. J. Lumin.*, 2023, 44(11): 2011-2026. (in Chinese)

[12] YAO L C, ZHOU X H, LU W, *et al.* Chemical potential effects on polytypism in Au-catalyzed GaAs nanowire molecular beam epitaxy growth: a first-principles study [J]. *Chem. Phys. Lett.*, 2016, 644: 147-151.

[13] KUSCH P, GRELICH E, SOMASCHINI C, *et al.* Type-Ⅱ band alignment of zinc-blende and wurtzite segments in GaAs nanowires: a combined photoluminescence and resonant Raman scattering study [J]. *Phys. Rev.* B, 2014, 89(4): 045310.

[14] ALEKSEEV P A, DUNAEVSKIY M S, ULIN V P, *et al.* Nitride surface passivation of GaAs nanowires: impact on surface state density [J]. *Nano Lett.*, 2015, 15(1): 63-68.

[15] 王鹏华, 唐吉龙, 亢玉彬, 等. GaAs纳米线晶体结构及光学特性[J]. 物理学报, 2019, 68(8): 087803.
WANG P H, TANG J L, KANG Y B, *et al.* Crystal structure and optical properties of GaAs nanowires [J]. *Acta Phys. Sinica*, 2019, 68(8): 087803. (in Chinese)

[16] YU T H, YAN L, YOU W, *et al.* The effect of passivation on different GaAs surfaces [J]. *Appl. Phys. Lett.*, 2013, 103(17): 173902.

[17] CHEN X, XIA N, YANG Z Y, *et al.* Analysis of the influence and mechanism of sulfur passivation on the dark current of a single GaAs nanowire photodetector [J]. *Nanotechnology*, 2018, 29(9): 095201.

[18] LIN A, SHAPIRO J N, SENANAYAKE P N, *et al.* Extracting transport parameters in GaAs nanopillars grown by selective-area epitaxy [J]. *Nanotechnology*, 2012, 23(10): 105701.

[19] TAJIK N, PENG Z, KUYANOV P, *et al.* Sulfur passivation and contact methods for GaAs nanowire solar cells [J]. *Nanotechnology*, 2011, 22(22): 225402.

[20] CRETÌ A, PRETE P, LOVERGINE N, *et al.* Enhanced optical absorption of GaAs near-band-edge transitions in GaAs/AlGaAs core-shell nanowires: implications for nanowire solar cells [J]. *ACS Appl. Nano Mater.*, 2022, 5(12): 18149-18158.

[21] FRANCAVIGLIA L, FONTANA Y, CONESA-BOJ S, *et al.* Quantum dots in the GaAs/Al_xGa_{1-x}As core-shell nanowires: Statistical occurrence as a function of the shell thickness [J]. *Appl. Phys. Lett.*, 2015, 107(3): 033106.

[22] 崔建功, 张霞, 颜鑫, 等. GaAs纳米线及GaAs/In_xGa_{1-x}As/GaAs纳米线径向异质结构的无催化选区生长的实验研究[J]. 物理学报, 2014, 63(13): 136103.
CUI J G, ZHANG X, YAN X, *et al.* Selective-area growth of GaAs and GaAs/In_xGa_{1-x}As/GaAs nanowires by MOCVD [J]. *Acta Phys. Sinica*, 2014, 63(13): 136103. (in Chinese)

[23] CAROFF P, DICK K A, JOHANSSON J, *et al.* Controlled polytypic and twin-plane superlattices in Ⅲ-V nanowires [J]. *Nat. Nanotechnol.*, 2009, 4(1): 50-55.

[24] KETTERER B, HEISS M, UCCELLI E, *et al.* Untangling the electronic band structure of wurtzite GaAs nanowires by resonant Raman spectroscopy [J]. *ACS Nano*, 2011, 5(9): 7585-7592.

[25] KANG Y B, NA G R, WANG D K, *et al.* Controlled synthesis of pure-phase GaAs nanowires through shear tension [J]. *ACS Photonics*, 2021, 8(10): 2889-2897.

[26] PATRIARCHE G, GLAS F, TCHERNYCHEVA M, *et al.* Wurtzite to zinc blende phase transition in GaAs nanowires induced by epitaxial burying [J]. *Nano Lett.*, 2008, 8(6): 1638-1643.

[27] LOITSCH B, RUDOLPH D, MORKÖTTER S, *et al.* Tunable quantum confinement in ultrathin, optically active semiconductor nanowires *via* reverse-reaction growth [J]. *Adv. Mater.*, 2015, 27(13): 2195-2202.

[28] 夏宁, 方铉, 王登魁, 等. GaAs一维纳米结构生长控制及表面改性方面的研究进展[J]. 电子世界, 2018(4): 53-55.
XIA N, FANG X, WANG D K, *et al.* Research progress in growth control and surface modification of GaAs one-dimensional nanostructures [J]. *Electron. World*, 2018(4): 53-55. (in Chinese)

[29] WANG S, LI H L, TANG J L, *et al.* Crystal phase control in self-catalyzed GaAs nanowires grown on pre-etched Si substrates [J]. *Mater. Adv.*, 2023, 4(18): 4250-4257.

[30] SPIRKOSKA D, ARBIOL J, GUSTAFSSON A, *et al.* Structural and optical properties of high quality zinc-blende/wurtzite GaAs nanowire heterostructures [J]. *Phys. Rev.* B, 2009, 80(24): 245325.

[31] LAUTENSCHLAGER P, GARRIGA M, LOGOTHETIDIS S, *et al.* Interband critical points of GaAs and their tempera-

ture dependence [J]. *Phys. Rev.* B, 1987, 35(17): 9174-9189.

[32] SUN H D, CALVEZ S, DAWSON M D, *et al*. Thermal quenching mechanism of photoluminescence in 1.55 μm GaInNAsSb/Ga(N)As quantum-well structures [J]. *Appl. Phys. Lett.*, 2006, 89(10): 101909.

[33] LI H L, CHEN Y T, WEI Z P, *et al*. Optical property and lasing of GaAs-based nanowires [J]. *Sci. China Mater.*, 2020, 63(8): 1364-1381.

[34] OUATTARA L, MIKKELSEN A, SKÖLD N, *et al*. GaAs/AlGaAs nanowire heterostructures studied by scanning tunneling microscopy [J]. *Nano Lett.*, 2007, 7(9): 2859-2864.

张志宏(1995-),男,甘肃兰州人,博士研究生,2018年于长春理工大学获得学士学位,主要从事低微材料光电器件的研究。

E-mail: zhihongzhang@um.edu.mo

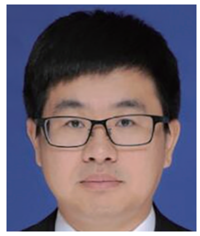

魏志鹏(1978-),男,吉林长春人,博士,教授,博士生导师,2008年于中国科学院长春光学精密机械与物理研究所获得博士学位,主要从事半导体光电子器件方面的研究。

E-mail: weizp@cust.edu.cn

亢玉彬(1991-),男,河南商丘人,博士,硕士生导师,2022年于长春理工大学获得博士学位,主要从事低微材料生长及低微材料光电子器件的研究。

E-mail: kangyubin@cjlu.edu.cn